Scattering, loss, and gain of surface plasmons

Beijnum, F. van

Author: Beijnum, Frerik van
Title: Scattering, loss, and gain of surface plasmons
Issue Date: 2013-05-15

Chapter 6

Loss compensation of extraordinary optical transmission

Surface plasmons offer many new possibilities in photonics, but applications are often limited by absorption or radiative loss. Compensating these losses will further improve the applicability of surface plasmons. In this context, long range surface plasmons have been successfully amplified [93, 94], and amplified spontaneous emission of surface plasmons is reported [21, 95]. Simultaneously, various kinds of surface plasmon lasers [96] have been studied experimentally [12, 40, 97, 98]. Despite the large interest in surface plasmon lasers, lasing may also be a nuisance when improving a lossy metallic system. Such problems may occur in metamaterials [22], like negative index materials [79, 99, 100] or n=0 metamaterials [9]. Also metal hole arrays, known for their extraordinary optical transmission [28], could show unintended laser action which may be detrimental to their performance. In this chapter we show strong loss compensation in extraordinary optical transmission and identify a number of challenges in loss compensation of resonant plasmonic systems in general.

F. van Beijnum, P. J. van Veldhoven, E. J. Geluk, G. W. ’t Hooft, and M. P. van Exter, submitted for publication.

6.1 Introduction

The metal hole array is an ideal system to study loss compensation for several reasons. First, the extraordinary optical transmission (EOT) is thoroughly studied, see [43] for a recent review. Second, the role of surface plasmons in the EOT phenomenon is also quantitatively understood nowadays [36, 37]. Third, the EOT has potential applications, like biosensing [39, 101]. Last, EOT is also an example of a Fano resonance [102], often exploited in plasmonic nanostructures [103–106].

Figure 6.1 shows the essence of the experiment, which is measuring the optical transmission of a metal hole array that has a semiconductor (InGaAs) gain layer placed in close proximity of the metal. The gain layer is pumped optically with a 1064 nm laser beam. The experiment is performed in a Helium flow cryostat to increase the potential gain of the semiconductor. The gain material can amplify the surface plasmons, which are excited at the holes, and thereby increase the optical transmission. The luminescence of the gain material is also transmitted through the holes and is emitted in all directions, which gives rise to background luminescence (red arrows).

6.2 Evolution with pump power

Figure 6.2 shows the key result of this chapter, namely the evolution of the transmission with pump power. The inset shows the transmission when the system is not pumped (red curve), with a transmission maximum of 8.6×10^{-3}. This spectrum shows the well-known Fano line shape. The dashed grey curve shows the estimated transmission in the absence of any surface waves, which is 2.3×10^{-3} at 1500 nm. Hence the transmission of the unpumped system is enhanced by a factor 3.7 by the presence of surface waves.

When we increase the pump power the maximum transmission increases

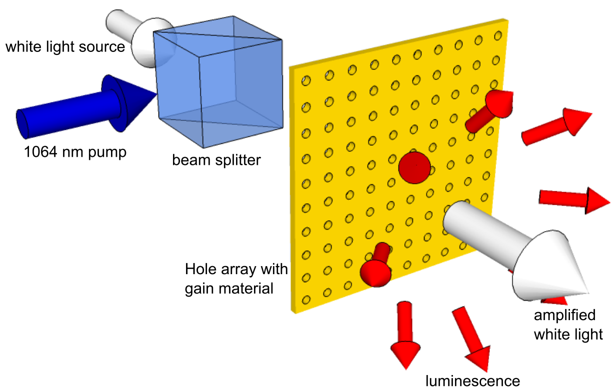

Figure 6.1: A sketch of the experiment. We record the white light transmission spectrum of a hole array that has a gain layer in close proximity of the metal, while pumping the gain layer with a laser. The luminescence from the pumped gain material is also recorded (red arrows).

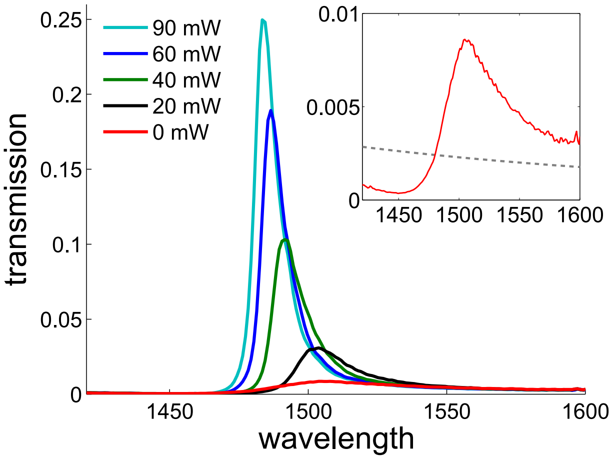

Figure 6.2: Measured transmission as a function of pump power. The transmission maximum gradually increases with pump power from 8.6×10^{-3} (see inset) to 0.25, which is a 31 fold enhancement. The lattice spacing of this sample is $a_0 = 450$ nm; 90 mW corresponds to roughly 7kW/cm^2

dramatically, while it remains practically constant at other wavelengths. At 90 mW pump power, the transmission has reached a value of 0.25, corresponding to a 31 fold increase of the transmission. The transmission enhancement as a result of surface waves is now 109, instead of 3.7. As a reference, in a recent experiment without loss compensation we found an 17 fold enhancement for a hole array on glass [37]. Hence we conclude that loss compensation can dramatically increase the EOT.

6.3 Background luminescence

In Fig. 6.3 we show that the increased transmission is indeed due to amplification of the incident white light, because at the transmission maximum the transmitted intensity is much larger than the background luminescence. The transmission plotted here is $T = (I_{out} - I_{bg})/I_{in}$, where I_{in} is the incident white light intensity, I_{bg} is the background signal when only the pump is switched on, and I_{out} is the intensity recorded when both light sources are on. The background luminescence plotted in Fig. 6.3 is I_{bg} divided by the value of I_{in} at 1490 nm. We have also studied the background luminescence at an angle where the white light is absent, to check that the background is not affected by switching the white light source on.

At the transmission minimum the background signal exceeds the transmitted signal, which imposes a challenge on measuring the transmission minimum accurately. To limit this problem, the light source used in a loss compensated transmission experiment has to be sufficiently bright. Here, we use a superluminescent diode, which is much brighter than the halogen lamp that is generally used for EOT experiments.

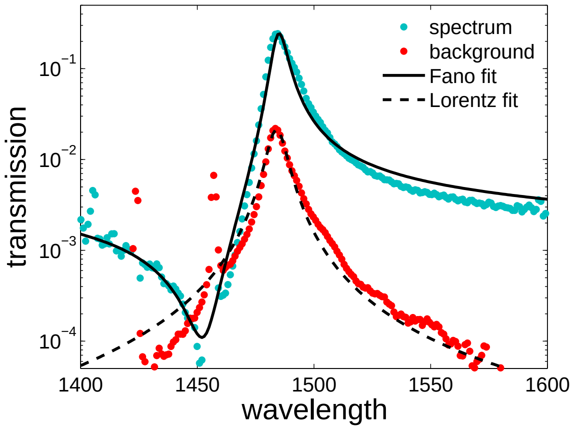

Figure 6.3: Comparison between the collected background luminescence and the transmitted white light. At the transmission maximum, the background luminescence is an order of magnitude smaller. At the transmission minimum, however, the magnitude of the background luminescence exceeds that of the transmitted white light. Please note that the plots are on a semilog scale.

We fitted the background luminescence using a Lorentzian lineshape, which describes the luminescence to good approximation. The resonance wavelength and spectral width of the Lorentzian is the same as that of the Fano resonance that is fitted to the transmission spectrum. This shows that both resonances have the same origin, namely surface waves propagating on the metal dielectric interface.

The background luminescence in Fig. 6.3 exhibits two narrow linewidth resonances, at $\sim$ 1425 nm and $\sim$ 1460 nm. These are resonances with a subradiant character [107]. We have recently shown that such resonances can show laser action. Fortunately, this laser emission is donut shaped and therefore it has limited emission normal to the surface where we measure the transmission. Nonetheless, this laser action may hinder loss compensation in two ways. First, the lasing peak will largely exceed the transmitted signal and therefore subtraction of the background may become inaccurate. Second, when the device starts lasing the gain of the semiconductor will not increase anymore with a further increase of pump power, because all additional pump power is lost to the lasing mode [21, 108]. Hence, these two narrow linewidth resonances exemplify that loss compensation can lead to lasing effects at one wavelength that hinder further loss compensation at other wavelengths [22].

6.4 Quantitative analysis

We now compare the transmission enhancement for a set of three different samples with different lattice spacings a_0: 470, 460 and 450 nm, of which the 450 nm sample is discussed in Figs. 6.2 and 6.3. This quantitative analysis will address two questions: What limits the observed enhancement? How much gain is supplied by the semiconductor material? The transmission spectra of

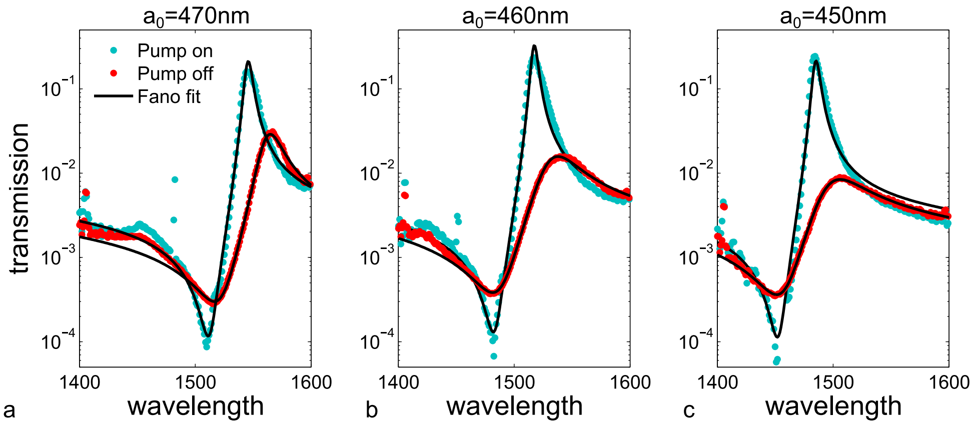

Figure 6.4: Transmission for samples of different lattice spacing: $a_0 = 470$ nm (**a**), 460 nm (**b**), and 450 nm (**c**). The transmission at maximum pump power (90 mW) is compared to that without pumping. The data is fitted to a Fano resonance.

these three samples are plotted on a semilog scale in Figs. 6.4a, 6.4b and 6.4c, where the spectra with the pump on and off are compared. Each sample is pumped strong enough to be close to full inversion within the bandwidth of the Fano resonances. Noteworthy is that the transmission at the minimum decreases in presence of the pump, showing that pumping can also decrease the transmission.

The six smooth curves in Fig. 6.4 are Fano fits to the data. Our Fano expression is an approximate version of the microscopic model for EOT, which is recently developed [36] and verified [37]. The expression for these fits is as follows:

$$T = \left| t\omega^2 + \frac{\alpha\omega^4}{\omega - \omega_0 + i\gamma} \right|^2 \tag{6.1}$$

The parameter t is proportional to the transmission in absence of any surface wave, α quantifies the combined excitation and outcoupling, which also has a phase difference with respect to t, ω_0 is the resonance frequency and γ is the combined ohmic and radiative loss of the surface plasmon. For convenience we expressed ω, ω_0 and γ in eV.

In Table 6.1 we show the key fit values for the three plots in Fig. 6.4, comparing the pumped and unpumped resonances. For the unpumped samples, this linewidth increases with decreasing lattice parameter. This is as expected: at reduced wavelengths the absorption losses in the gold and the unpumped gain medium increase, while also the scattering losses induced by the holes increase. For the pumped samples, the increased ohmic and radiative losses

Table 6.1: Fit parameters corresponding to the Fano fits in Fig. 6.4. Dimensions of λ_0 and $\Delta\lambda$ are nm, and eV^{-4} and eV^{-2} for $|\alpha|$ and t, respectively

Parameter	λ_0	$\Delta\lambda$	$\|\alpha\|$	t
470 nm, off	1562	12	2.8×10^{-3}	73×10^{-3}
470 nm, on	1545	4	2.4×10^{-3}	87×10^{-3}
460 nm, off	1530	20	2.7×10^{-3}	80×10^{-3}
460 nm, on	1517	4	2.5×10^{-3}	90×10^{-3}
450 nm, off	1494	24	2.1×10^{-3}	70×10^{-3}
450 nm, on	1485	4	2.1×10^{-3}	81×10^{-3}

could explain that the linewidth does not become smaller than 4 nm.

The difference between the pumped and unpumped linewidth is the gain experienced by the surface plasmon. This difference increases more than a factor two from 8 to 20 nm when a_0 decreases. The 20 nm difference can be converted into the net gain that is experienced by the surface plasmon using:

$$\frac{4\pi n_{\text{eff}}}{\lambda^2}\left(\Delta\lambda_{off} - \Delta\lambda_{on}\right) = L_{off}^{-1} - L_{on}^{-1} \tag{6.2}$$

where L_{off} and L_{on} are the effective propagation lengths without and with pump, respectively. The difference $L_{off}^{-1} - L_{on}^{-1}$ of 3.5×10^3 cm^{-1} for the $a_0 = 450$ nm sample, is the change in inverse absorption length of the surface waves. To relate it to the material gain, this value needs to be divided by the confinement factor, estimated to be 0.32 for our system. For a conservative estimate of the material gain at this wavelength and at full inversion, we also have to divide $L_{off}^{-1} - L_{on}^{-1}$ by two. Hence, the estimated material gain is 5.5×10^3 cm^{-1} for the 450 nm sample and 2.2×10^3 cm^{-1} for the 470 nm sample. These numbers are reasonable for a semiconductor operated at high carrier densities and low temperatures [97, 109].

The parameter α, which models the excitation and outcoupling of the surface plasmons shows little dependence on pump power for each sample. This shows that the measured enhancement and the spectral width are consistent, and in agreement with $T_{max} \approx |\alpha|^2\omega^8/\gamma^2$. The parameter t is also more or less constant for all six cases, as expected for the nonresonant transmission.

Finally, we note that there is much room for improvement of our results, for example by carefully maximizing the thickness of the gain layer, placing the gain layer closer to the metal interface, or using quantum wells. The system would also become more practical when electrical pumping is implemented and when the structures can be operated at room temperature.

6.5 Conclusion

We have demonstrated the improved performance of a plasmonic system using a semiconductor gain material. We increase the transmission of a metal hole array by a factor 31. Our quantitative analysis shows that we experimentally obtain the large but expected material gain. Three challenges are identified that are generic to loss compensation in plasmonic systems: (1) subtraction of the background luminescence can be troublesome; (2) to observe any transmission signal, the signal beam needs to be sufficiently intense compared to the background luminescence; (3) gain saturation will occur when the structure lases unintentionally. Therefore, loss compensated systems need to be designed with much care, taking the physics of the gain medium and optical resonances into account.

6.6 Methods

The sample is fabricated as follows. On a semi-insulating indium phosphide wafer a lattice-matched indium gallium arsenide layer is grown (105 nm), which is subsequently covered with a thin (15 nm) layer of indium phosphide. Hereafter a 5 nm protective silicon nitride layer is grown using plasma enhanced chemical vapor deposition. On these layers we fabricate the metal hole array by depositing 100 nm gold and 20 nm titanium on a lithographically defined array of dielectric pillars. To provide sufficient adhesion of the gold onto the silicon nitride, we deposit a very thin (average thickness smaller than 0.5 nm) titanium adhesion layer in between these layers. The last step is to etch the pillars away, leaving the subwavelength holes (diameter 160 nm).

The setup for transmission measurements is as follows. We illuminate the sample with two beams, at the sample the pump beam is roughly 40 μm diameter and the white light signal roughly 12 μm diameter. To create a pump spot of uniform intensity we illuminated a pinhole with the pump laser, and imaged this pinhole on the sample. The diameter of this pinhole is roughly two times smaller than that of the laser beam. The signal beam is generated using a superluminescent diode with a center wavelength of 1550 nm and a spectral width of 110 nm. The transmitted light is collected using a microscope objective. The far field of the objective is imaged onto a single mode fiber, which is subsequently led to a grating spectrometer with a linear array. The angular resolution of the setup is $\sim$ 4 mrad. This low angular resolution helps to minimize the collected laser emission from the hole arrays.

Because the sample is placed inside a cryostat, we can not move the sample in and out of the beam without changing the alignment. For this reason we use the signal at unperforated areas of the sample as a reference. Later, we measure the transmission spectra of the unpumped samples outside the cryostat to determine the correct prefactor for the transmission measurement.